I ENCIT - Rio de Janeiro, RJ (Dez. 1986)

TRANSPORT COEFFICIENTS FOR LAMINAR AND TURBULENT FLOW THROUGH A FOUR-CUSP CHANNEL

ABCM
ABENS

ALEXANDRE DE SOUZA DUTRA
JOSÉ ALBERTO DOS REIS PARISE
PAULO ROBERTO DE SOUZA MENDES

Departamento de Engenharia Mecânica - PUC/RJ

PUC/RJ

ABSTRACT

A comprehensive study was performed to determine entrance region and fully-developed heat transfer coefficients for laminar and turbulent flow in a four-cusp channel. A numerical solution was presented for fully-developed laminar flow, and an experimental study was reported for turbulent flow. Systematic variations of the Reynolds number were made in the range 900-30000. The results show that the heat transfer coefficients for the four-cusp channel are much lower than the coefficients for the circular tube.

INTRODUCTION

Simulation of accidents in nuclear reactors is a fundamental practice when a criterious study to enhance safety of the nuclear plants is desired. Such practice is only possible when related heat transfer information is available.

The four-cusp channel appears when the cylindrical shells of the fuel swell during the accident, touching each other.

A number of papers on four-cusp channel flow is available in the literature. Gunn and Darling [1] performed a numerical and experimental study on the hydrodynamical problem. Later, some numerical studies on the laminar flow and heat transfer were reported in [2] and [3].

The present paper deals mainly with an experimental investigation on the heat transfer characteristics of the turbulent flow in a four-cusp channel. In the experiments, the naphthalene sublimation technique was employed. For completeness, a numerical solution of the laminar flow was also performed, as described in the following section of the paper.

NUMERICAL SOLUTION

The calculation domain is depicted in Figure 1. It is clear that, due to symmetry, only one eighth of the channel cross section needs to be analyzed. The numerical solution presented here pertains to the case of fully-developed, constant-property flow through the channel under study.

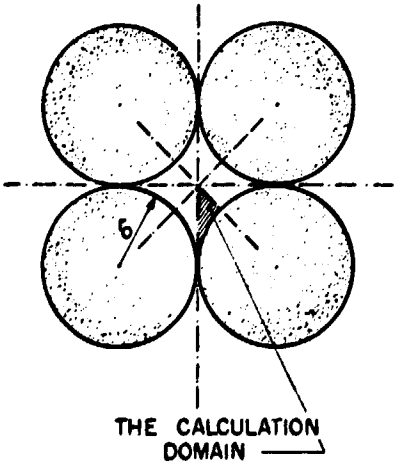

Figure 1. The four-cusp channel

The momentum and energy equations take the usual dimensionless form

$$\partial^2\Omega/\partial R^2 + (\partial^2\Omega/\partial\theta^2)/R^2 + 1 = 0 \qquad (1)$$

$$\partial^2\phi/\partial R^2 + (\partial^2\phi/\partial\theta^2)/R^2 + (\Omega/\overline{\Omega})\lambda\phi = 0 \qquad (2)$$

In eq.(1), the dimensionless velocity Ω is defined as $w\mu/(-dp/dz)D_h^2)$, where w denotes the axial velocity in the z direction, p is the pressure, μ is the absolute viscosity and D_h is the hydraulic diameter, whose definition is well known. The quantity R is the dimensionless radial coordinate, defined as r/D_h (see Figure 1); and θ is the angular coordinate.

In eq.(2), $\phi \equiv (T-T_w)/(T_b-T_w)$ is the dimensionless temperature, where T_w is the channel wall and T_b is the bulk temperature. The constant λ is defined as $(-d(T_b-T_w)/dZ)/(T_b-T_w)$, where Z is the dimensionless axial coordinate, given by $(z/D_h)/Pe$. The quantity Pe is the Peclet number, given by the product between the Reynolds number $Re \equiv \rho\overline{w}D_h/\mu$ and the Prandtl number $Pr \equiv \mu c_p/K$.

Since λ is not known a priori, a subsidiary equation is needed. For this purpose, the nondimensional counterpart of the definition of the bulk temperature is employed,

$$\iint \phi\Omega\, RdRd\theta / \overline{\Omega} = 1 \qquad (3)$$

The boundary conditions for eq.(1) are the no-slip condition ($\Omega = 0$) at the wall ($R = a$), and symmetry conditions ($\partial\Omega/\partial n = 0$) at the other boundaries. An isothermal wall boundary condition ($\phi = 0$) is imposed at $R = a$ for eq.(2), whereas, at the other boundaries, the symmetry condition ($\partial\phi/\partial n = 0$) applies. In the above relations $a = \pi/2(4-\pi)$.

The friction factor $f \equiv 2(-dp/dz)D_h/\rho\overline{w}^2$ is calculated via

$$f = 2/\overline{\Omega}\,Re\ . \qquad (4)$$

It can be easily shown that the average Nusselt number $\overline{Nu} = \overline{h}D_h/K$, where K is the thermal conductivity, is given by

$$\overline{Nu} = \lambda/4\ , \qquad (5)$$

whereas the local Nusselt number $Nu = hD_h/K$ is evaluated by

$$Nu = -(\partial\phi/\partial R)_{R=a} \qquad (6)$$

The symbols h and $\overline{h}$ stand respectively for the local and average heat transfer coefficients.

As implied by the above equations, cylindrical coordinates were employed. Therefore, the channel wall is a line of constant R, whereas the symmetry line normal to the wall is a line of constant θ. On the other hand, the third boundary of the calculation domain is not parallel to any of the coordinates.

Equations (1) and (2) were integrated via the finite-volume technique described in [4]. A non-uniform 92×92 grid was employed, and the irregularity of the domain was tackled with the technique presented in [5].

THE EXPERIMENTS

The naphthalene sublimation technique was chosen for the determination of the heat transfer coefficients. This technique for determining heat transfer coefficients is based on the existing analogy between heat and mass transfer phenomena, offers higher accuracy, better control of boundary conditions and minimal extraneous losses. The thermal boundary condition for the heat transfer situation which is analogous to the actual mass transfer situation is uniform wall temperature.

Test Section. The test section is made up of interlocking modules, as illustrated in Figure 2. Each module consists of a cylindrical metallic (brass) shell whose inner surface is coated with a layer of solid naphthalene. The coating is applied in one module at a time by a casting procedure which is well outlined in [6]. In this manner, after the modules are assembled together, a four-cusp channel with pure naphthalene walls is obtained. Precise mating of successive modules is ensured by interlocking recesses and giding pins that are provided at the respective ends of each module.

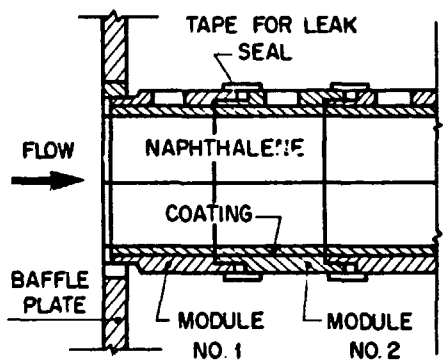

Figure 2. The test section

Air Loop. The test section was situated at the upstream end of the open-loop flow circuit that was operated in the suction mode. Air was drawn into the inlet of the test section from the temperature-controlled laboratory room. From the test section exit, the air entered a flow metering section (an orificie-plate calibrated meter), then followed to a plenum chamber, to a cut-off valve, to a control valve, and then to blower. The purpose of the plenum chamber was to dampen oscillations of the air flow induced by the blower. The blower was situated in an adjacent room to avoid thermal and naphthalene contamination.

The test section was oriented horizontally and was built into a large baffle plate. The pressure of the baffle created a plenumlike space upstream of the inlet from which the test section drew the air.

Instrumentation. Mass measurements were made using a Sartorius analytical balance with a resolving power of 10^{-4} g and a capacity of 200 g.

During the casting procedure, a thermocouple was embedded in the naphthalene coating of a module, in such a way that its junction was positioned flush with the channel wall. This module was always positioned at the downstream end of the test section. The thermocouple was made of from specially calibrated copper-constantan wire.

Periodic readings of the thermocouple emf were made during the course of a data run with the aid of a voltmeter having a 1 μV resolution.

Experimental Procedure. It was standard practice to leave the naphthalene-coated modules in the temperature-controlled laboratory overhight, in order to attain thermal equilibrium with the room air. During this period, the modules were kept in a sealed plastic bag to avoid sublimation and also to ensure that the air in the room was free of naphthalene vapor.

Immediately prior to a data run, the modules were individually weighed and then assembled to form the test section. The blower had been warmed up in preparation for the run, so that it provided a steady flow from the moment of its activation. After the pre-selected derivation of the run, the test section was disassembled and the modules reweighed. During all of these operations, the modules were never touched with bare hands; rather, either gloves or padded ongs were used.

To obtain a correction for possible extraneous sublimation which might have occurred between the two weighings, a so-called after-run was made. During the after-run, all aspects of the actual data run were repeated, except that the blower was never activated, and there was no airflow period. Further weighing following the after-run provided the sought-for correction, which was of the order of one percent.

NUMERICAL RESULTS

The numerical solution of the laminar fully developed flow through the four cusp channel is now presented. The ratio between maximum and mean velocity in the cross section was found to be equal to 2.38, whereas the product f.Re, evaluated numerically via eq.(4), was found to be equal to 26.3.

Figure 3 shows the Nusselt number distribution along the wall. It can be seen from this figure that the region in the neighborhood of the cusp is nearly inactive as far as heat transfer is concerned. Departing from the cusp ($\theta > 15^{\circ}$), the local Nusselt number increases very fast, showing a maximum value of 3.59 at $\theta = 45^{\circ}$. The average Nusselt number was found to be equal to 1.08 and this result agrees well with [2] and [3]. It is worth noting that the average Nusselt number predicted by the simple relation given in Figure 3.7 of [7] is equal to 1.00 for this geometry.

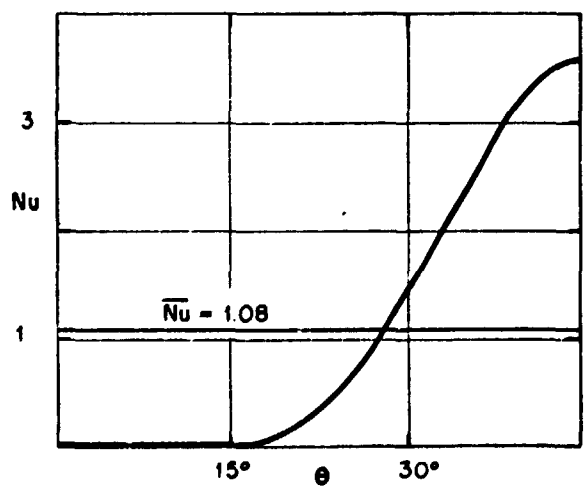

Figure 3. Local Nusselt number for laminar flow

EXPERIMENTAL RESULTS

The mass transfer coefficients and Sherwood numbers obtained in the experiments can be converted to heat transfer coefficients by employing the analogy between the two processes. Because of this, the phrases heat transfer and mass transfer will be used

interchangeably in the presentation of results.

Data Reduction. The per-module mass transfer coefficient, K_i, for a typical module, i, was evaluated from the defining equation

$$K_i = (\dot{M}_i/A_w) / \Delta\rho_{n,i} \qquad (7)$$

In this equation, $\dot{M}_i$, the per-module mass transfer rate, was obtained from the ratio $\Delta M_i/\tau$, where ΔM_i is the measured (and corrected) change in the module mass and τ is duration of the run.

The quantity $\Delta\rho_{n,i}$ is the wall-to-bulk difference in naphthalene vapor density for module i. Its evaluation requires that the axial variation of the bulk vapor density, ρ_{nb}, first be determined. For this purpose, let j denote any module in the test section, with ρ_{nb}^{j-1} representing the bulk vapor density at the inlet of the module and ρ_{nb}^{j} representing the bulk vapor density at the module exit. Then, noting that $\rho_{nb}=0$ at the test section inlet, a mass balance in the channel yields

$$\rho_{nb}^{i} = \sum_{j=1}^{i} \dot{m}_j / (m/\rho) \qquad (8)$$

where $\dot{m}$ is the measured mass flow rate, and ρ is the mean air density at the section.

The other ingredient needed for the evaluation of the wall-to-bulk density difference is the naphthalene vapor density, ρ_{nw}, at the channel wall. This quantity was obtained by a two-step process. First, by using the measured wall temperature, the naphthalene vapor pressure at the wall was calculated by the Sogin vapor pressure/ /temperature equation [8]. Then, ρ_{nw} was evaluated from the perfect gas law.

Two definitions of the wall-to-bulk difference in vapor density were considered: the arithmetic - mean difference and the log-mean difference. For all the experiments, the per-module rise in bulk density was small compared with the wall-to-bulk density difference and, hence, the two definitions yielded indistinguishable results. The log-mean difference was used in the data reduction because it is conventional practice in the heat transfer literature.

$$\Delta\rho_{n,i} = \{(\rho_{nw}-\rho_{nb}^{i-1}) - (\rho_{nw}-\rho_{nb}^{i})\} / \ln\{(\rho_{nw}-\rho_{nb}^{i-1}) / (\rho_{nw}-\rho_{nb}^{i})\} \qquad (9)$$

The dimensionless counterpart of the mass transfer coefficient is the Sherwood number Sh_i, defined as

$$Sh_i = (K_i D_h/\nu)Sc \qquad (10)$$

where the Schmidt number Sc is equal to 2.5 for naphthalene diffusion in air. The kinematic viscosity ν was evaluated as that for pure air.

ENTRANCE REGION RESULTS

The axial distribution of the Sherwood number is given in Figure 4 for some representative values of the Reynolds number. A more complete presentation is available in [6]. In the figure, the per-module Sherwood number is plotted as a function of the dimensionless axial coordinate z/D_h. In particular, the Sherwood for each module is plotted at the axial midpoint of the module, and the data for the different Reynolds numbers are identified by different symbols.

From this figure, it is seen that the flow is fully developed after about five hydraulic diameters for Re = 5300, after about seven hydraulic diameters for Re = 14800, and after about eight hydraulic diameters for Re = 30300. Qualitatively, the trends shown in Figure 4 are the same ones found in flows through any channel whose cross section does not vary along its length.

Fully Developed Results. As observed in Figure 4, the Sherwood number tends to an asymptotic value in the region far away from the channel inlet. These fully developed values of Sh are plotted in Figure 5 as a function of the Reynolds number. The figure suggests that this fully developed value of the per module Sherwood number Sh_{fd} has a dependence on the Reynolds number of the power-law type. A least-squares fit to these data yields

$$Sh_{fd} = 0.0645\ Re^{0.672} . \qquad (11)$$

The well known Dittus-Boelter equation is also plotted (for Pr = Sc = 2.5) in Figure 5. A comparison between the two curves readily yields that the four-cusp channel displays a much poorer performance as far as heat transfer is concerned. This is an expected behavior, since a large portion of the heat transfer area is in the neighborhood of a cusp, where very low fluid velocities prevail.

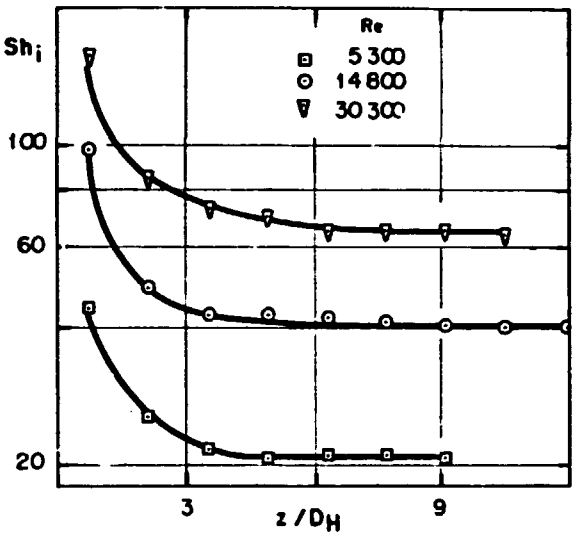

Figure 4. Effect of Reynolds number on the axial distributions of the Sherwood number

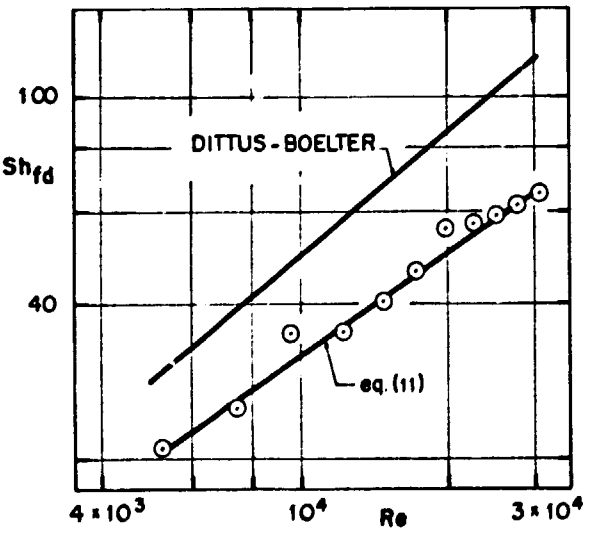

Figure 5. Effect of Reynolds number on the fully-developed Sherwood number

FINAL REMARKS

The research described here constitutes a comprehensive study of the laminar and turbulent heat transfer characteristics of the four cusp channel. For laminar flow, a numerical solution was presented, whereas an experimental analysis was described for turbulent flow.

The results showed that the heat transfer coefficients of the four-cusp channel are always lower than the ones for the circular tube. For laminar flow, the Nusselt number was found to be only three tenths of Nu for the circular tube, whereas for turbulent flow this ratio is not as low in the range investigated, but increases with the Reynolds number.

REFERENCES

[1] Gunn, D.J. and Darling, C.W.W., Fluid flow and energy losses in non-circular conduits. Trans. Instn. Chem. Engrs., 41 : 163-173 (1963).

[2] Maliska, C.R. and Silva, A.F.C., Local effects of highly nonorthogonal grids in the solution of heat transfer problems in cusped corners. Proc. 1st Intl. Conference on Num. Grid Generation in Comp. Fluid Dynamics, West Germany, July 1986.

[3] Nieckele, A.O., Análise do escoamento laminar com transferência de calor em um canal quadri-cúspide. Relatório nº 011/86, LNCC/CNPq, Julho 1986.

[4] Patankar, S.V., Numerical heat transfer and fluid flow. McGraw-Hill, New York (1980).

[5] Patankar, S.V., A numerical method for conduction in composite materials, flow in regular geometries, and conjugate heat transfer. Proc. 6th Intl. Heat Transfer Conference, Toronto, v.3, pp. 297-304, (1978).

[6] Dutra, A.S., Coeficientes de transporte em dutos de seção quadricúspide simulando o núcleo danificado de um reator nuclear. M.S.Thesis, Mech. Eng. Dept., Pontifícia Universidade Católica do Rio de Janeiro (Mar 1985).

[7] Bejan, A., Convection heat transfer. John Wiley & Sons, New York (1984).

[8] Sogin, H.H., Sublimation from disks to air streams flowing normal to their surfaces. Trans. ASME 80, pp.61-71 (1958).